

## Roman-Subaru/HSC Concurrent Observations for Rogue Planet Mass Measurements

DAISUKE SUZUKI,<sup>1</sup> WILLIAM DEROCOCCO,<sup>2,3</sup> KANSUKE NUNOTA,<sup>1</sup> DAVID BENNETT,<sup>2,3</sup> SCOTT GAUDI<sup>4</sup> AND SEAN TERRY<sup>2,3</sup>  
ON BEHALF OF ROMAN GALACTIC EXOPLANET SURVEY PROJECT INFRASTRUCTURE TEAM (RGES-PIT)

<sup>1</sup>*Department of Earth and Space Science, Graduate School of Science, Osaka University, Osaka 560-0043, Japan*

<sup>2</sup>*Department of Astronomy, University of Maryland, College Park, MD 20742, USA*

<sup>3</sup>*Code 667, NASA Goddard Space Flight Center, Greenbelt, MD 20771, USA*

<sup>4</sup>*Department of Astronomy, The Ohio State University, 140 West 18th Avenue, Columbus, OH 43210, USA*

### ABSTRACT

We propose Roman-Subaru/HSC concurrent observations of the Roman Space Telescope’s Galactic Bulge Time Domain Survey (GBTDS) field to measure the mass of free-floating rogue planets (FFPs). We request at least 200 hours (20 nights assuming 10 hours per night) of HSC observations, with which we expect to detect  $\approx 20$  FFPs in HSC data. In conjunction with Roman’s photometric data, these detections will allow a direct measurement of each FFP’s mass. The statistical data of measured/constrained FFP mass and transverse velocity will be key to understanding the underlying mechanisms that drive planetary formation, migration, and ejection. Only such data can test a predicted pebble isolation mass in circumbinary systems. Concurrent observations of the same FFP microlensing event by Roman and another telescope are necessary to measure the mass of the FFP lens. Subaru/HSC is the best instrument in the world for this purpose. Concurrent HSC observations will also significantly reduce false positive contamination among Roman’s FFP candidate events, which will be a significant challenge during Roman’s initial observational seasons. Furthermore, these concurrent observations will enable mass measurements of bound planets as well. Roman-HSC concurrent observations would strongly enhance the science outcome of the GBTDS, and, with Roman’s finite operational lifetime, this is an opportunity upon which we should maximize before it goes away.

### 1. SUMMARY OF NEEDS

Only through concurrent, high-cadence photometric observations of microlensing events by Roman and another telescope can one measure the masses of the free-floating planets (FFPs). The mass-measured FFP sample can answer the fundamental questions about how FFPs are ejected from their birth systems and the dynamical processes that sculpt planetary systems in their early stages. Subaru/HSC is the best facility/instrument to perform these concurrent observations with Roman, given the good natural seeing, wide field-of-view, and high quality and throughput of the instrument. We propose  $z$ -band high cadence observations toward Roman’s GBTDS field as shown in Fig. 1 when Roman is observing the field. We request at least 200

hours of HSC observations, with which we expect to detect  $\approx 20$  FFP events (See Fig. 1).

### 2. INTRODUCTION

Free-floating planets (FFPs) are planetary mass objects that do not orbit host stars. It is not clear how FFPs are formed. Massive FFPs would be formed through a similar process to brown dwarf/low mass star formation. Alternatively, FFPs could be formed through the same processes as bound planets and kicked out of their birth system by their interactions with other planets/host star(s) in that system or other stars passing nearby. If very massive FFPs are still young, they can be detected by imaging method as they emit thermal flux (Miret-Roig et al. 2022). Unfortunately, the vast majority FFPs are too faint for imaging. Gravitational microlensing is the only method that can detect such FFPs (Johnson et al. 2020).

FFP microlensing events have a short timescale,  $t_E < 2$  days, compared to the typical value of  $t_E \sim 20$  days for stellar microlensing events toward the Galactic bulge, as

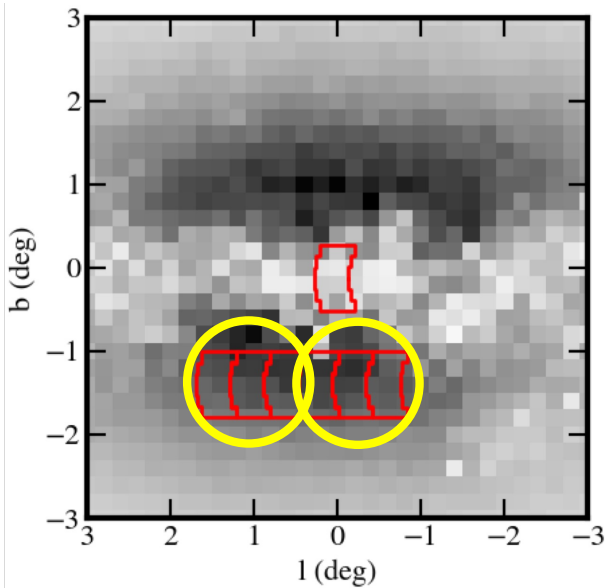


**Figure 1.** The expected HSC footprints in yellow circles cover the Roman GBTD field (red). The plotted Roman field is the nominal survey design recommended by the GBTD Definition Committee. The dust extinction of the Galactic center field is too high for the HSC  $z$ -band so we focus on the bulge fields.

$t_E$  scales to  $\sqrt{M}$ , where  $M$  is the lens mass. Earth-mass FFPs show a few hours of magnification (see Fig. 2), so high-cadence ( $> 1$  per 1 hour) imaging is required to capture these FFP microlensing events.

The Roman GBTD is expected to detect 200-1000 FFPs depending on the assumed FFP mass function (Johnson et al. 2020; Sumi et al. 2023). One of the survey capability requirements of Roman’s GBTD is “EML 2.0.4: Roman Space Telescope shall be capable of measuring the frequency of free floating planetary mass objects in the Galaxy from Mars to 10 Jupiter masses. If there is one  $M_{\text{Earth}}$  free floating planet per star, measure this frequency to better than 25%” (RST-SYS-REQ-0020, Revision D 2023). However, a measurement of the masses of FFPs is impossible with Roman data alone. To measure the mass of FFPs, one needs to detect both finite source and microlensing parallax effects in very short timescale events. Due to the short timescale, the microlensing parallax signal can only be detected by concurrent observations with Roman and another telescope (Fig. 2, top panel). As indicated in the bottom panel of Fig. 2, both finite source and microlensing parallax detection give us two independent mass-distance relations ( $\theta_E$  and  $\pi_E$ ) and the overlap of these curves gives us the mass of and distance to the FFP.

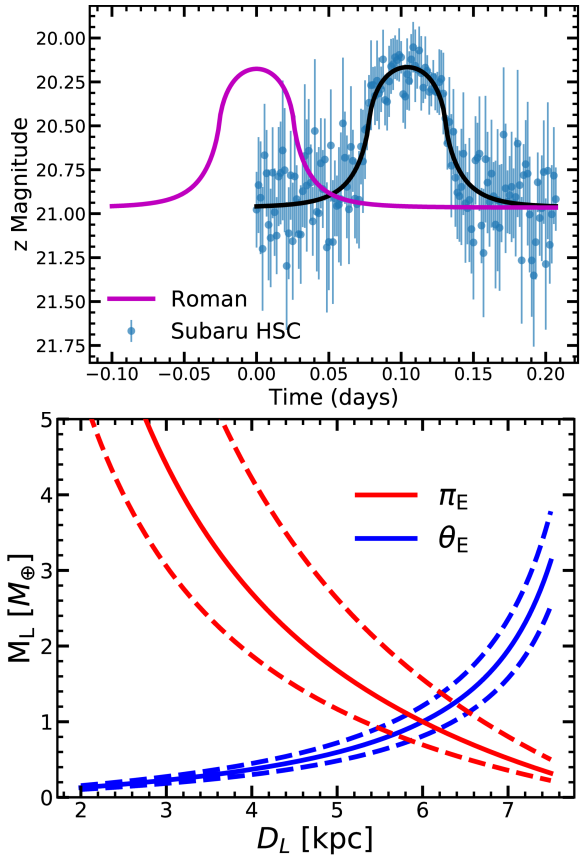


**Figure 2.** Top: The expected HSC  $z$ -band light curve of an Earth-mass FFP. The rounded shape of the peak of the magnification is the finite source effect which allows us to measure the angular Einstein radius,  $\theta_E$ . The offset of the peak time (and magnification) between the Roman and HSC light curves is due to the microlensing parallax effect (Udalski et al. 2015), with which the microlensing parallax parameter,  $\pi_E$ , can be determined. Bottom: The mass and distance relations of  $\theta_E$  and  $\pi_E$  for a 1 Earth mass FFP at 6 kpc from us.

### 3. FFP MASS MEASUREMENT IS KEY TO UNDERSTANDING PLANET FORMATION

So far, three independent ground-based microlensing surveys have found evidence of an FFP population (Gould et al. 2022; Koshimoto et al. 2023; Mróz et al. 2017, 2018, 2019, 2020a,b; Sumi et al. 2011). Recently, Sumi et al. (2023) derived the FFP mass function based on the 9 year MOA survey as shown in Fig. 3. This result indicates that the number of FFPs may be upwards of  $\sim 20$  times the number of bound cold planets. This is a remarkable result that strongly motivates dedicated work on FFPs, however their prediction for the abundance of low-mass FFPs is subject to considerable uncertainty, as they restricted their functional form to

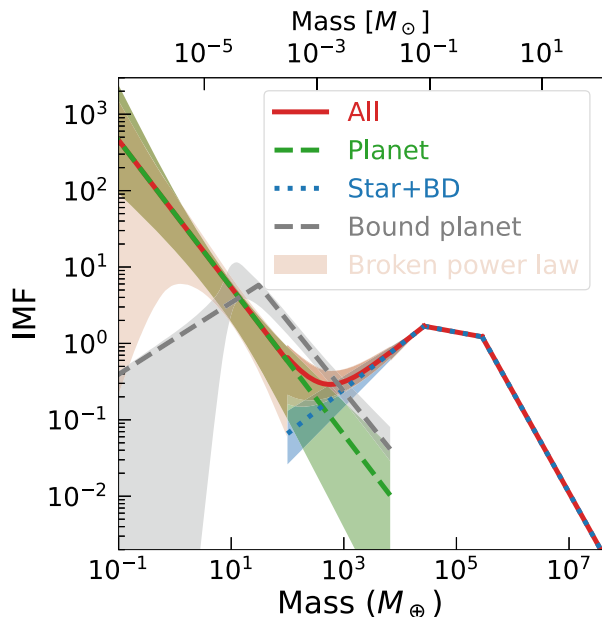


**Figure 3.** IMF of the best fit model to the MOA 9-yr data sample from Sumi et al. (2023) (Figure 6 of their paper).

a single-power or broken-power law for the FFP mass function. Also note that they assumed that the velocity dispersion of FFPs is the same as that of stars. Critically, *the mass of each FFP was not measured*; instead, the authors fit for the overall mass function based in a Bayesian frame work, which depends on the assumed models and prior.

On the other hand, a theoretical study, Coleman & DeRocco (2025) predicts an FFP mass function based on marginalizing over the relative contributions of multiple formation pathways and stellar populations from a large suite of simulations. As indicated in Fig. 4, this theoretical model predicts a peak at  $\sim 8M_{\oplus}$ , which is the pebble isolation mass. This peak is due to a unique feature of planet formation in circumbinary systems that are expected to produce most FFPs. Protoplanetary disks in circumbinary systems have a central cavity where gravitational interactions with the binary stars severely deplete the disk. This causes planets at the pebble isolation mass that are migrating inward to halt their migration, and begin a planet-planet gravitational scattering process that ends up ejecting many planets through interactions with one of the host stars. So, the discovery of such a feature would provide evidence in favor of the pebble accretion model that would not be available without a precise measurement of the FFP mass function. Unfortunately, current observational results do not

probe sufficiently low masses to constrain such a feature well.

Indeed, it is critical to greatly enhance the observational data quality and/or statistics to constrain FFP formation models, and as a result, planetary formation theory as a whole. First, we need to increase the statistics. We need more detections of FFP microlensing events. This is one of the Roman’s GBTDS science requirements, so this will be achieved by Roman’s high spatial resolution and high cadence data. Secondly, even more importantly, we need to obtain a sample of *mass-measured FFPs*. This will greatly enhance FFP science because it will allow us

- to confirm whether they are truly planetary mass objects and eliminate false positives,
- to investigate the FFP mass distribution without any assumption, and
- to put constraints on the transverse velocity of and distance to each FFP.

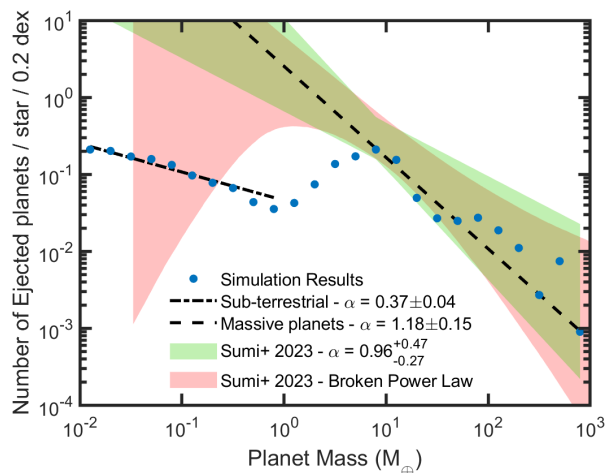


**Figure 4.** The predicted FFP mass function from Coleman & DeRocco (2025) (Figure 4 in their paper).

Direct measurements of the FFP masses enable the reconstruction of the true FFP mass function without the need for an assumed Galactic model and functional form. Such measurements can be used to directly test theoretical predictions and enable the determination of the dynamical processes leading to FFP formation. A sample of the measurements and constraints on the transverse velocity of FFPs will have additional important information as well, because it is expected that the different planet ejection processes result in different excess velocities Coleman & DeRocco (2025). So both

mass and transverse velocity measurement of FFPs can constrain the FFP ejection mechanism, which is impossible by any other observational means. By accounting for both bound and unbound planets we can comprehensively constrain the planet formation model for the first time.

#### 4. CONCURRENT OBSERVATIONS CAN RULE OUT THE FALSE POSITIVES

If we detect a candidate for a short microlensing event, we need to assess whether it is real or not. Cataclysmic variable stars (CVs), flare stars, heartbeat stars, other source of stellar variability, and solar system bodies such as Kuiper belt objects (KBOs) can mimic short timescale microlensing events, posing a large observational challenge during Roman’s initial seasons. Concurrent observations by HSC have the ability to eliminate these false positives in two ways:

1. Multi-wavelength light curve data may show that the magnitude of the brightening is wavelength dependent, whereas the magnification of microlensing events is inherently achromatic. The HSC concurrent observation will be conducted with z-band, so we can get the color information automatically as the Roman data is mostly in the W146 filter.
2. Any detection of the microlensing parallax effect in the data (e.g., Fig. 2) would imply that the event *must* be a real microlensing event. False positives associated with any kind of stellar variability would not exhibit such an effect.

Therefore, HSC data can significantly reduce false positive events.

Even if a short timescale event is a real microlensing event, there is a possibility that the planet orbits its host with a wide enough separation so that the host star magnification does not show up in the observed light curve, i.e., the planet is a wide orbit planet, instead of FFP. Although the ground-based microlensing survey (with natural seeing) cannot distinguish whether the event is

due to a FFP or wide orbit planet, Roman GBTDs can do so as the spatial resolution is high enough to resolve the possible lens star flux. Even in this case, the microlensing parallax and finite source detection by the Roman-HSC concurrent observation is critical to measure the masses of the wide orbit small planet and its host.

#### 5. WHY SUBARU HSC?

We cannot predict when and where FFP microlensing events will occur and high-cadence observation is necessary to catch the shortest timescale events associated with the largely unexplored low-mass range of FFPs. Therefore, an instrument with a wide field-of-view and very high cadence is required. For this purpose, the FOV of ULTIMATE-Subaru/WFI ( $14' \times 14'$ ) is not wide enough and total survey efficiency (including overhead) is not optimal. HSC’s wider FOV ( $\phi = 1.5^\circ$ ) and high cadence make it a better choice for this task.

While the Galactic bulge is more visible from the southern hemisphere, the Vera Rubin Observatory is significantly less flexible than Subaru, and the Blanco telescope (with DECam) has a smaller primary mirror than Subaru.

OGLE, MOA, and KMTNet, the three primary ground-based microlensing surveys, are expected to observe the Roman field, but they are 1-2m class telescope and natural seeing is very limited. Fig. 5 compares the detection efficiency of short microlensing events in MOA (Koshimoto et al. 2023) and Subaru/HSC. The HSC simulation is based on the 5-hour light curves with 8 minutes cadence, with which we expect about 20 FFP detections with 200 hours of the HSC observations. The H-band microlensing survey of PRIME would have an advantage in the regions with high dust extinction, but the Roman’s GBTDs field does not show very high extinction.

Therefore, Subaru/HSC is the best instrument in the world to perform the simultaneous observations, providing the first opportunity to measure the masses of, and by extension explore the origins of these rogue worlds.

#### REFERENCES

- Coleman, G. A. L., & DeRocco, W. 2025, MNRAS, 537, 2303, doi: [10.1093/mnras/staf138](https://doi.org/10.1093/mnras/staf138)
- Gould, A., Jung, Y. K., Hwang, K.-H., et al. 2022, Journal of Korean Astronomical Society, 55, 173, doi: [10.5303/JKAS.2022.55.5.173](https://doi.org/10.5303/JKAS.2022.55.5.173)
- Johnson, S. A., Penny, M., Gaudi, B. S., et al. 2020, AJ, 160, 123, doi: [10.3847/1538-3881/aba75b](https://doi.org/10.3847/1538-3881/aba75b)
- Koshimoto, N., Sumi, T., Bennett, D. P., et al. 2023, AJ, 166, 107, doi: [10.3847/1538-3881/ace689](https://doi.org/10.3847/1538-3881/ace689)
- Miret-Roig, N., Bouy, H., Raymond, S. N., et al. 2022, Nature Astronomy, 6, 89, doi: [10.1038/s41550-021-01513-x](https://doi.org/10.1038/s41550-021-01513-x)
- Mróz, P., Udalski, A., Skowron, J., et al. 2017, Nature, 548, 183, doi: [10.1038/nature23276](https://doi.org/10.1038/nature23276)

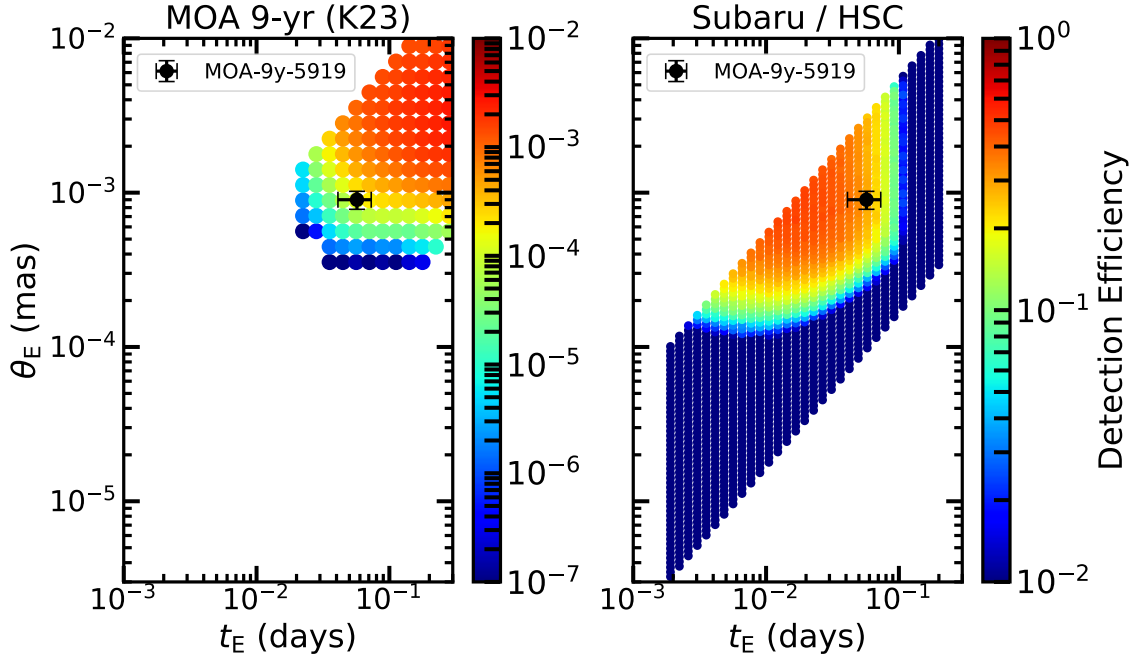


**Figure 5.** Detection efficiency of the FFP microlensing events for the MOA-II survey (left) and simulated Subaru/HSC light curve (right). The detection threshold of  $\Delta\chi^2 = 25$  between the flat and single lens model is used for the detection of the magnification. The diagonal shape is limited by the lens-source relative proper motion of  $0.6 < \mu_{\text{rel}}(\text{mas/yr}) < 20$ , where  $\mu_{\text{rel}} = \theta_E/t_E$ . The black circle with error bars shows the Earth mass FFP candidate, MOA-9y-5919. The detection efficiency of this event with HSC is higher than the MOA data by three orders of magnitude.

Mróz, P., Ryu, Y. H., Skowron, J., et al. 2018, *AJ*, 155, 121, doi: [10.3847/1538-3881/aaaae9](https://doi.org/10.3847/1538-3881/aaaae9)

Mróz, P., Udalski, A., Bennett, D. P., et al. 2019, *A&A*, 622, A201, doi: [10.1051/0004-6361/201834557](https://doi.org/10.1051/0004-6361/201834557)

Mróz, P., Poleski, R., Han, C., et al. 2020a, *AJ*, 159, 262, doi: [10.3847/1538-3881/ab8aeb](https://doi.org/10.3847/1538-3881/ab8aeb)

Mróz, P., Poleski, R., Gould, A., et al. 2020b, *ApJL*, 903, L11, doi: [10.3847/2041-8213/abbfad](https://doi.org/10.3847/2041-8213/abbfad)

RST-SYS-REQ-0020, Revision D. 2023,

[https://roman.gsfc.nasa.gov/science/docs/RST-SYS-REQ-0020D\\_DOORs\\_Export.pdf](https://roman.gsfc.nasa.gov/science/docs/RST-SYS-REQ-0020D_DOORs_Export.pdf)

Sumi, T., Kamiya, K., Bennett, D. P., et al. 2011, *Nature*, 473, 349, doi: [10.1038/nature10092](https://doi.org/10.1038/nature10092)

Sumi, T., Koshimoto, N., Bennett, D. P., et al. 2023, *AJ*, 166, 108, doi: [10.3847/1538-3881/ace688](https://doi.org/10.3847/1538-3881/ace688)

Udalski, A., Yee, J. C., Gould, A., et al. 2015, *ApJ*, 799, 237, doi: [10.1088/0004-637X/799/2/237](https://doi.org/10.1088/0004-637X/799/2/237)